



## Characterization of anion exchange fiber for simultaneous removal of Cr(VI) and As(V) in mineral processing wastewater

Seung-Chan Lee<sup>a</sup>, Jin-Kyu Kang<sup>a</sup>, Nag-Choul Choi<sup>a</sup>, Chang-Gu Lee<sup>b</sup>, Song-Bae Kim<sup>a,c,\*</sup>

<sup>a</sup>Environmental Functional Materials and Water Treatment Laboratory, Seoul National University, Republic of Korea, email: kn5102@snu.ac.kr (S.-C. Lee), naengie@snu.ac.kr (J.-K. Kang), nagchoul@empas.com (N.-C. Choi)

<sup>b</sup>Department of Environmental and Safety Engineering, Ajou University, Republic of Korea, email: changgu@ajou.ac.kr (C.-G. Lee)

<sup>c</sup>Department of Rural Systems Engineering and Research Institute of Agriculture and Life Sciences, Seoul National University, Republic of Korea, Tel. +82-2-880-4587, email: songbkim@snu.ac.kr (S.-B. Kim)

Received 22 May 2018; Accepted 24 September 2018

### ABSTRACT

In this study, a modacrylic anion exchange fiber (Karacaron™ SA2) made from acrylonitrile and vinyl chloride was used for the removal of Cr(VI) and As(V) in aqueous solutions. This study focused on the two parts: (i) investigate the simultaneous removal of Cr(VI) and As(V) present in mineral processing wastewater by the SA2, and (ii) examine the protonated amine sites available on the SA2 in response to pH change using X-ray photo electron spectroscopy (XPS) analysis. Batch experiments indicated that the maximum removal capacities for Cr(VI) and As(V) were 2.350 and 0.346 mmol/g, respectively. The SA2 was successfully regenerated by 0.1 M NaCl solution and reused for five adsorption-desorption experiments. The removal of Cr(VI) and As(V) was influenced by the solution pH. The pH dependency of Cr(VI) and As(V) removal was closely related to both the number of protonated amines available for anion exchange and speciation of Cr(VI) and As(V) in response to the pH change. XPS analysis demonstrated that the C-N<sup>+</sup> peak (401.5 eV) was prominent at pH 2. As pH increased to 4 and 10, the C-N<sup>+</sup> peak gradually decreased due to partial deprotonation of the anion exchange sites. At pH 12, the C-N<sup>+</sup> peak disappeared because nearly all of the exchange sites were deprotonated. Simultaneous removal experiments in mineral processing wastewater (pH = 2.9; Cr(VI) concentration = 60.2 mmol/L; As(V) concentration = 67.5 mmol/L) demonstrated that Cr(VI) removal by the SA2 tended to be greater than that of As(V). The Cr(VI) and As(V) removal capacities in the wastewater were 1.587–3.098 and 0.042–2.124 mmol/g, respectively, at fiber dosages of 2–20 g/L.

*Keywords:* Anion exchange fiber; Arsenate; Chromate; Ion exchange; Mineral processing wastewater

### 1. Introduction

Industrial waste waters are generated from various industrial activities including paper manufacturing, textile industries, mining, oil and gas industries, iron and steel industries, and food industries [1]. Inorganic and organic contaminants in industrial waste waters are released into water environments, polluting valuable water resources and resulting in serious health problems. Chromium (Cr) and arsenic (As) are two representative contaminants found

in industrial waste waters. Chromium waste water can be discharged into water environments from industrial activities such as electroplating, leather tanning, dyeing, and textiles [2]. In water environments, trivalent Cr (III) is insoluble and less dangerous, whereas hexavalent Cr(VI) is extremely soluble and highly toxic [3]. Arsenic wastewater can be released into aquatic environments from mining-related activities. Both trivalent As (III) and pentavalent As(V) are soluble in water environments. As (III) (arsenite) exists in reducing environments and is more toxic and soluble than As(V) (arsenate), which is predominant in oxidizing conditions [4].

\*Corresponding author.

Anion exchange is a treatment technique used to separate anionic contaminants (Cr(VI) and As(V)) in waste water via exchange with anions (chloride and hydroxide) on the surface of anion exchange resins or anion exchange fibers. Many studies have analyzed the removal of Cr(VI) or As(V) in aqueous solutions using anion exchange resins [5–17]. Compared to anion exchange resins, anion exchange fibers have higher ion exchange capacity and faster sorption rate [18]. Several studies have researched the removal of Cr(VI) or As(V) with anion exchange fibers [19–26] and demonstrated that anion exchange fibers can successfully remove Cr(VI) or As(V) from aqueous solutions. However, studies related to the simultaneous removal of Cr(VI) and As(V) in industrial wastewater using anion exchange fibers are scarce.

In this study, an anion exchange fiber was used for the removal of Cr(VI) and As(V) in aqueous solutions. This study focused on the two parts: (i) investigate the simultaneous removal of Cr(VI) and As(V) present in mineral processing wastewater by the anion exchange fiber, and (ii) examine the protonated amine sites available on the anion exchange fiber in response to pH change using X-ray photo electron spectroscopy (XPS) analysis. Batch removal experiments were conducted to examine the influences of solution pH, regeneration, kinetic, equilibrium, and competing anions on the removal of Cr(VI) and As(V) in synthetic solutions. Furthermore, batch experiments were performed to investigate the simultaneous removal of Cr(VI) and As(V) in the wastewater.

## 2. Materials and methods

### 2.1. Characterization of the anion exchange fiber

The anion exchange fiber (Karacaron™ SA2) was used as received from the manufacturer (Kaneka Corporation, Osaka, Japan). The SA2 is a modacrylic anion exchange fiber made from acrylonitrile and vinylchloride [27]. Field emission scanning electron microscopy (FESEM, Supra 55VP, Carl Zeiss, Oberkochen, Germany) was used to obtain microscopic images of the SA2, from which the average diameter was quantified using the Image J 1.43u software (National Institutes of Health, Bethesda, MD, USA). energy dispersive X-ray (EDX) spectrometer analysis was also performed using FESEM to determine the elemental composition. Fourier-transform infrared (FTIR) spectrometer (Nicolet 6700, Thermo Scientific, Waltham, MA, USA) was used to generate the spectra of the fiber before and after the removal experiments. XPS (Sigma Probe, Thermo VG, East Grinstead, UK) scans with monochromatic Al K $\alpha$  radiation were also conducted before and after the removal experiments. The volumetric anion exchange capacity of the fiber was quantified following the procedures reported in the literature [28]. First, 0.3 g of the fiber was immersed in 1 M hydrochloric acid (HCl) solution for 6 h and dried at 65°C in a drying oven (Thermo Stable SOF-W 155, Daihan Scientific, Seoul, Korea). Then, the fiber was soaked in a 300 mL solution of 5% Na<sub>2</sub>SO<sub>4</sub>, which was shaken for 180 min at 30°C and separated from the fiber. The chloride ion concentration was then measured using ion chromatography (ICS-3000, Dionex, Sunnyvale, CA, USA).

### 2.2. Removal experiments for Cr(VI) and As(V) in synthetic solution

Removal experiments for Cr(VI) were performed in triplicate under batch conditions (solution volume = 300 mL; temperature = 30°C). The Cr(VI) stock solution was prepared from potassium dichromate (K<sub>2</sub>Cr<sub>2</sub>O<sub>7</sub>) dissolved in deionized water. The pH experiment was performed at solution pHs of 2–12 (initial Cr(VI) concentration = 0.882 mmol/L; fiber dose = 1.0 g/L; reaction time = 180 min). The solution pH was adjusted with 0.1 M HCl and 0.1 M NaOH. The flasks were shaken at 150 rpm using a shaking incubator (Daihan Science, Seoul, Korea). The solution samples were collected through centrifugation and the Cr(VI) concentrations were analyzed using inductively coupled plasma-atomic emission spectroscopy (ICP-AES) (Optima-4300, Perkin Elmer, Waltham, MA, USA). The removal rate (%) and removal capacity (mmol/g) were calculated as follows:

$$\text{Removal rate} = \frac{C_i - C_f}{C_i} \times 100 \quad (1)$$

$$\text{Removal capacity} = \frac{C_i - C_f}{a} \quad (2)$$

The kinetic experiment was conducted at reaction times of 0–180 min (initial Cr(VI) concentration = 0.192 mmol/L; fiber dose = 20 g/L; solution pH = 5.1). The equilibrium experiment was performed at initial Cr(VI) concentrations of 0.192–19.23 mmol/L (solution pH = 4.3–5.1; fiber dose = 1.0 g/L; reaction time = 180 min). The competing anion experiments were conducted (initial Cr(VI) concentration = 0.882 mmol/L; fiber dose = 1.0 g/L; reaction time = 180 min) in the binary mixtures with a molar ratio of ([competing anion]/[Cr(VI)]) = 1. The competing anions included chloride (Cl<sup>-</sup>), nitrate (NO<sub>3</sub><sup>-</sup>), sulfate (SO<sub>4</sub><sup>2-</sup>), and phosphate (HPO<sub>4</sub><sup>2-</sup>). The relative removal reduction (Re, %) for Cr(VI) was calculated using the following relationship:

$$\text{Re} = \left( 1 - \frac{q_w}{q_{w/o}} \right) \times 100 \quad (3)$$

The regeneration experiment was conducted using a 0.1 M NaCl solution as the regenerant (initial Cr(VI) concentration = 0.882 mmol/L; fiber dose = 1.0 g/L; solution pH = 5.1; reaction time = 180 min). After the removal experiments, the fiber was immersed into the regenerant, which was shaken for 60 min at 150 rpm for the desorption of adsorbed Cr(VI) ions. Then, the regenerated fiber was dried for 2 h at 65°C in a drying oven prior to reuse.

Removal experiments for As(V) were also conducted under batch conditions. The As(V) stock solution was prepared from sodium arsenate dibasic heptahydrate (Na<sub>2</sub>HAsO<sub>4</sub>) dissolved in deionized water. The pH experiment was performed at initial As(V) concentration of 0.882 mmol/L and solution pHs of 2–12. The kinetic experiment was conducted at reaction times of 0–180 min (initial As(V) concentration = 0.192 mmol/L; fiber dose = 20 g/L; solution pH = 10.0). The equilibrium experiment was performed at initial As(V) concentrations of 0.067–6.674 mmol/L (solution pH = 7.5–8.6; fiber dose = 1.0 g/L; reaction time = 180 min). The competing anion experiments were conducted (initial As(V) concentra-

tion = 0.882 mmol/L; fiber dose = 1.0 g/L; reaction time = 180 min) in the binary mixtures with a molar ratio of ([competing anion]/[As(V)]) = 1. The value of  $Re$  was also calculated using Eq. (3). The regeneration experiment was conducted using a 0.1 M NaCl solution as the regenerant (initial As(V) concentration = 0.133 mmol/L; solution pH = 10.0; fiber dose = 1.0 g/L; reaction time = 180 min). The As(V) concentrations were analyzed using ICP-AES.

### 2.3. Removal experiments for Cr(VI) and As(V) in mineral processing wastewater

Simultaneous removal of Cr(VI) and As(V) by the SA2 in mineral processing wastewater was examined under batch conditions. The mineral processing wastewater used in the experiment is characterized in Table 1. Note that the Cr(VI) and As(V) concentrations in the wastewater were 60.2 mmol/L and 67.5 mmol/L, respectively. The batch tests were conducted at fiber dosages of 2–20 g/L (solution volume = 300 mL; reaction time = 180 min). The flasks were shaken at 150 rpm using a shaking incubator, and then solution samples were collected through centrifugation. The Cr(VI) and As(V) concentrations were analyzed using ICP-AES.

### 2.4. Model analysis

The equilibrium data were analyzed using the following equilibrium sorption models.

$$q_e = K_f C_e^{\frac{1}{n}} \quad \text{Freundlich} \quad (4)$$

$$q_e = \frac{Q_m K_L C_e}{1 + K_L C_e} \quad \text{Langmuir} \quad (5)$$

$$q_e = \frac{K_R C_e}{1 + a_R C_e^g} \quad \text{Redlich-Peterson} \quad (6)$$

Table 1  
Ionic composition of the mineral processing wastewater used in the experiments

Ion composition	Concentration (mmol/L)
As <sup>5+</sup>	67.5
Cr <sup>6+</sup>	60.2
Zn <sup>2+</sup>	57.9
Cu <sup>2+</sup>	2.3
Na <sup>+</sup>	212
K <sup>+</sup>	59.0
Cl <sup>-</sup>	10.2
Br <sup>-</sup>	14.5
NO <sub>3</sub> <sup>-</sup>	445
SO <sub>4</sub> <sup>2-</sup>	11.7
HPO <sub>4</sub> <sup>2-</sup>	5.1
pH	2.9
EC	23.7 mS/cm

The kinetic data were analyzed using the following kinetic sorption models.

$$q_t = q_e (1 - e^{-k_1 t}) \quad \text{Pseudo first-order} \quad (7)$$

$$q_t = \frac{k_2 q_e^2 t}{1 + k_2 q_e t} \quad \text{Pseudo second-order} \quad (8)$$

$$q_t = \frac{1}{\beta} \ln(\alpha\beta) + \frac{1}{\beta} \ln t \quad \text{Elovich} \quad (9)$$

The following equations for  $R^2$ ,  $\chi^2$ , and SAE were used to analyze the removal data and confirm their fit to the model.

$$R^2 = \frac{\sum_{i=1}^m (y_c - \bar{y}_e)_i^2}{\sum_{i=1}^m (y_c - \bar{y}_e)_i^2 + \sum_{i=1}^m (y_c - y_e)_i^2} \quad (10)$$

$$\chi^2 = \sum_{i=1}^m \left[ \frac{(y_e - y_c)_i^2}{y_c} \right] \quad (11)$$

$$SAE = \sum_{i=1}^n |y_c - y_e|_i \quad (12)$$

## 3. Results and discussion

### 3.1. FESEM and EDX

FESEM image (Fig. 1a) demonstrated that the SA2 was a micron-sized fiber, with a diameter of  $26.2 \pm 4.7 \mu\text{m}$ . The EDX spectra (Fig. 1b) demonstrated that carbon (C) was the major element of the fiber (atomic % of 66.65), with peak positions at 0.277 and 0.284 keV as  $K\alpha$  and  $K\beta$  signals, respectively. Oxygen (O) appeared at 0.523 and 0.532 keV as  $K\alpha$  and  $K\beta$  signals, respectively, due to amination in the aqueous solution. Nitrogen (N) was detected at 0.392 and 0.400 keV as  $K\alpha$  and  $K\beta$  signals, respectively, whereas chlorine (Cl) was evident at 2.622 keV as the  $K\alpha$  signal. N came from acrylonitrile ( $\text{C}_3\text{H}_3\text{N}$ ), whereas Cl came from vinyl chloride ( $\text{C}_2\text{H}_3\text{Cl}$ ). The volumetric anion exchange capacity of the fiber was determined to be 2.649 mmol/g.

### 3.2. FTIR spectra before and after the removal experiments

FTIR spectra of the SA2 are shown in Fig. 2. Before the removal experiments, amine groups (N–H) were detected at the peak of  $3249 \text{ cm}^{-1}$ , demonstrating that the fiber was functionalized through the amination reaction [29]. C–H vibration appeared at  $2921 \text{ cm}^{-1}$  in the fiber [30,31]. The peak at  $2243 \text{ cm}^{-1}$  corresponded to  $\text{C}\equiv\text{N}$  vibration from acrylonitrile [31], whereas the peak at  $677 \text{ cm}^{-1}$  was assigned to C–Cl vibration from vinyl chloride [32]. The peak at  $1637 \text{ cm}^{-1}$  corresponded to  $\text{O}=\text{C}-\text{N}-\text{H}$  (amide I), whereas the peak at  $1551 \text{ cm}^{-1}$  was assigned to  $\text{O}=\text{C}-\text{N}-\text{H}$  (amide II) [31,33].

In the FTIR spectra after Cr(VI) removal, Cr=O appeared at the peak of  $938 \text{ cm}^{-1}$ , whereas Cr–O was detected at the peak of  $755 \text{ cm}^{-1}$ , due to the interactions between Cr(VI) ions and anion exchange sites [34,35]. In the FTIR spectra after As(V) removal, an As–O vibration was found at the peak of  $842 \text{ cm}^{-1}$  [36], due to the association of As(V) ions with the exchange sites.

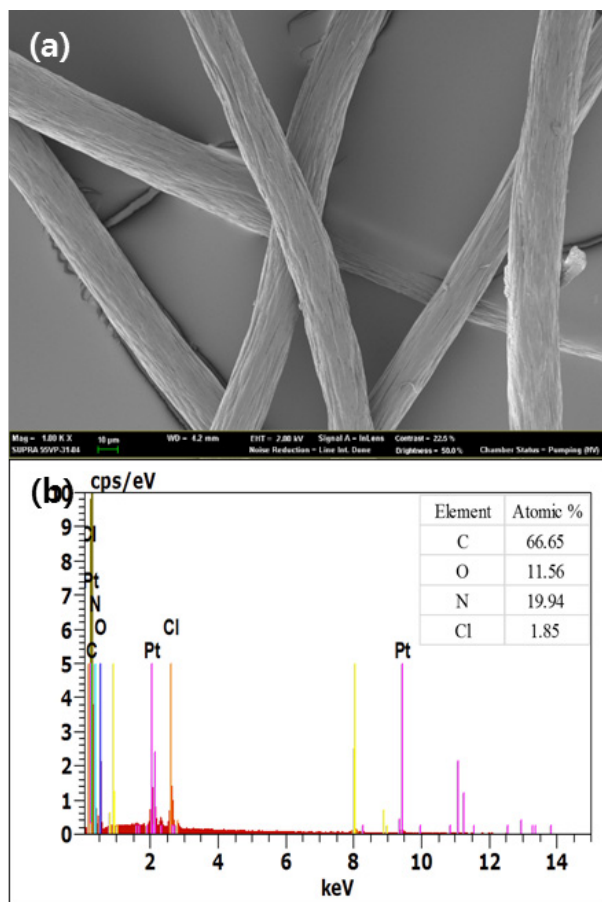


Fig. 1. Characteristics of the SA2: (a) FESEM image (bar = 10  $\mu\text{m}$ ) and (b) EDS pattern (inset = atomic %).

### 3.3. XPS spectra before and after the removal experiments

XPS spectra of the SA2 are shown in Fig. 3. In the wide scan before the removal experiments (Fig. 3a), the photo electron peaks at the binding energy of 285 and 532 eV were attributed to C1s and O1s, respectively. In addition, the peak at 398 eV was assigned to N1s, which came from the acrylonitrile. The peaks at 196 and 255 eV were assigned to Cl2p and Cl2s, respectively, which came from the vinyl chloride.

After the Cr(VI) removal experiments, the Cr2p peak appeared at 580 eV in the wide scan (Fig. 3c). In the high-resolution scan of the N1s region before the Cr(VI) removal (Fig. 3b), the peaks assigned to C $\equiv$ N and C–N were found at 399.2 and 400.5 eV, respectively, whereas the peak assigned to C–N $^+$  (protonated amine) appeared at 402.2 eV. After the Cr(VI) removal, the intensity of the C–N $^+$  peak decreased while the C–N peak increased (Fig. 3d). According to the high-resolution scan (Fig. 3e), the Cr2p region consisted of Cr2p $_{3/2}$  and Cr2p $_{1/2}$  spectra. The Cr2p $_{3/2}$  spectrum was centered at 577.0 eV, whereas the Cr2p $_{1/2}$  spectrum was at 586.6 eV. In the Cr2p $_{3/2}$  spectrum, the peaks assigned to Cr(III) and Cr(VI) were found at 576.8 and 579.0 eV, respectively, whereas the peaks assigned to Cr(III) and Cr(VI) appeared at 586.5 and 589.0 eV, respectively, in the Cr2p $_{1/2}$  spectrum.

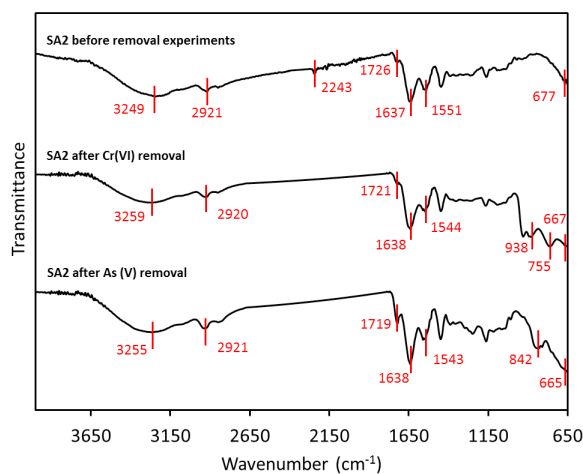


Fig. 2. FTIR spectra of the SA2 before and after the removal experiments.

These results could be attributed to the partial reduction of Cr(VI) to Cr(III) on the fiber after removal from aqueous solution. Researchers have reported that Cr(VI) species adsorbed on the surfaces of anion exchange fibers can be partially reduced to Cr(III) by electron-rich moieties on the surfaces of the anion exchange fibers [37,38].

After the removal of As(V), the As3d peak at 45 eV appeared in the wide scan (Fig. 3f). In the high-resolution scan of the N1s region (Fig. 3g), the C–N $^+$  and C–N peaks were slightly changed after the removal of As(V). These results demonstrate that protonated amine groups were responsible for the anion exchange of Cr(VI) and As(V).

### 3.4. Effect of pH on the removal of Cr(VI) and As(V)

The effect of solution pH on the removal of Cr(VI) and As(V) is presented in Fig. 4a, along with the speciation of Cr(VI) (Fig. 4b) and As(V) (Fig. 4c) in accordance with the pH change. These results showed that the removal of Cr(VI) and As(V) was influenced by the solution pH. At pH 2, the removal of As(V) behaved differently from that of Cr(VI). At pH 2, HCrO $_4^-$  was the major ionic form of Cr(VI) (Fig. 4b), and Cr(VI) was effectively removed by the fiber. However, As(V) removal at pH 2 was negligible because uncharged H $_3$ AsO $_4$  was the major ionic form of As(V) (Fig. 4c). Between pH 4 and 10, Cr(VI) and As(V) were effectively removed by the fiber. At pH 12, Cr(VI) and As(V) removal by the fiber were negligible. Our results also demonstrated that Cr(VI) removal by the fiber tends to be higher than that of As(V). Similar results were reported by Oliveira et al. [39], who demonstrated that Cr(VI) removal by leather waste was higher than As(V) removal at solution pHs of 2–6.

The effect of solution pH on the high-resolution scan in the N1s region in the XPS spectra is shown in Fig. 5. The pH dependency of Cr(VI) and As(V) removal could be closely related to the number of protonated amines available for anion exchange. XPS data demonstrated that the C–N $^+$  peak (401.5 eV) was prominent at pH 2. At highly acidic conditions, most of the anion exchange sites were protonated



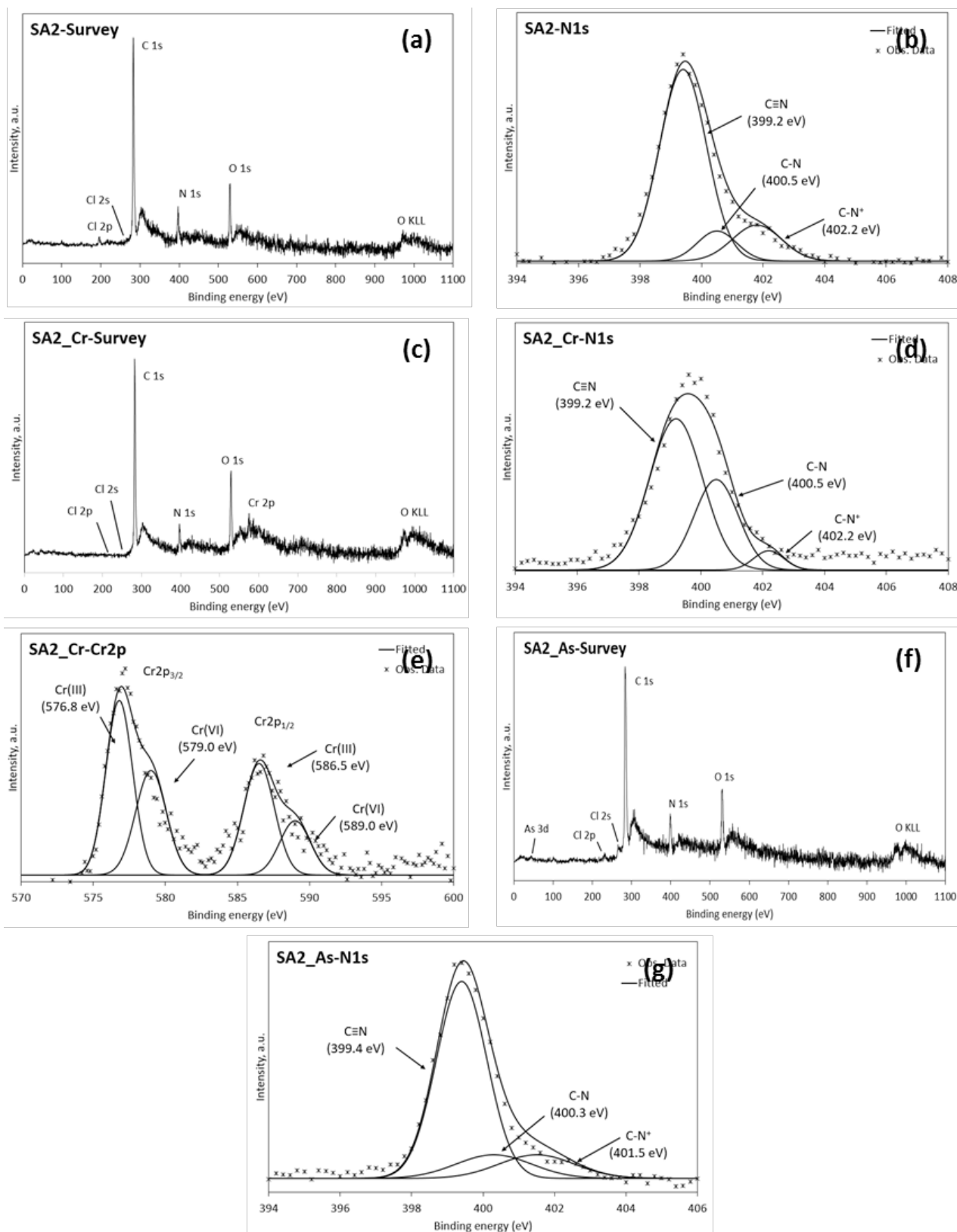


Fig. 3. XPS spectra of the SA2 before and after the removal experiments: (a) wide scan before the removal experiments, (b) high-resolution scan in the N1s region before the removal experiments, (c) wide scan after Cr(VI) removal, (d) high-resolution scan in the N1s region after Cr(VI) removal, (e) high-resolution scan in the Cr2p region after Cr(VI) removal, (f) wide scan after As(V) removal, and (g) high-resolution scan in the N1s region after As(V) removal.

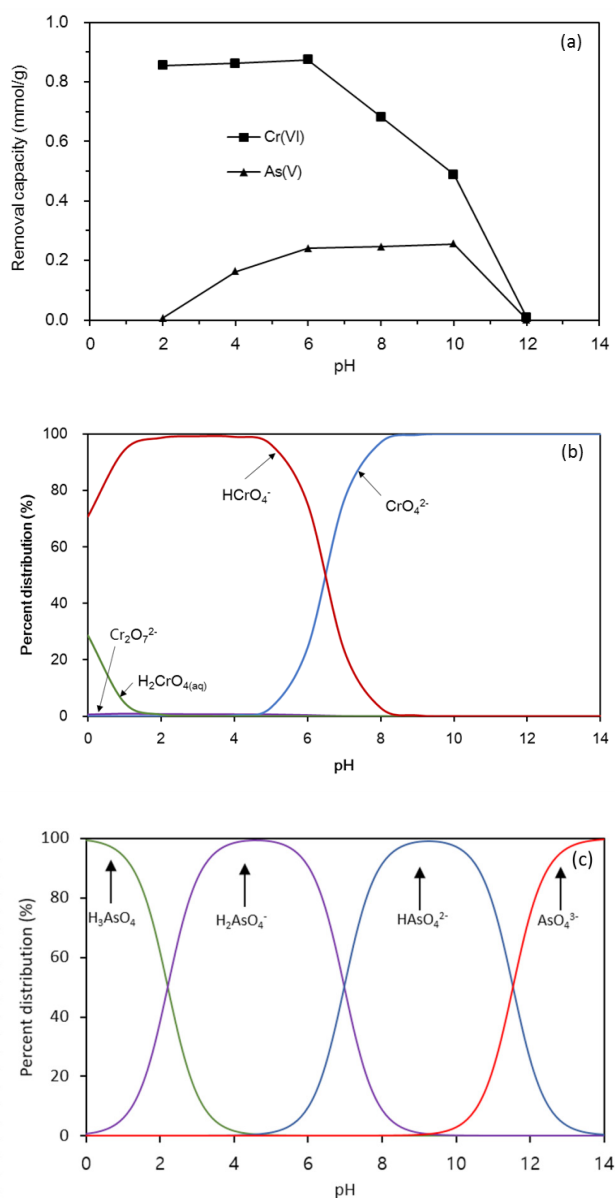


Fig. 4. Effect of solution pH on the removal of Cr(VI) and As(V) by the SA2: (a) removal capacity, (b) distribution of Cr(VI) species, and (c) distribution of As(V) species as a function of pH.

with exchangeable Cl ions; the amine functional groups on the fibers can be expressed as  $[\text{R}_2\text{NH}] \text{H}^+\text{Cl}^-$ . As pH increased to 4 and 10, the C-N<sup>+</sup> peak gradually decreased due to partial deprotonation of the anion exchange sites. At pH 12, the C-N<sup>+</sup> peak disappeared because early all of the exchange sites were deprotonated ( $[\text{R}_2\text{NH}]$ ).

### 3.5. Equilibrium, kinetic, competing anions, and regeneration analyses

Equilibrium sorption data were analyzed by the equilibrium models including the Freundlich [Eq. (4)], Langmuir [Eq. (5)], and Redlich-Peterson [Eq. (6)] isotherms. Equilib-

rium data along with the model fits for Cr(VI) and As(V) are presented in Figs. 6a and 6b, respectively. The corresponding model parameters are provided in Table 2. The values of  $R^2$ ,  $\lambda^2$ , and SAE indicated that the Freundlich model was better at describing the equilibrium data. The parameters values from the Freundlich model were  $K_F = 1.336 \text{ L/g}$  for Cr(VI) and  $K_F = 0.258 \text{ L/g}$  for As(V). Under the given experimental conditions, the maximum removal capacity for Cr(VI) quantified from the Langmuir model was one order of magnitude greater than that for As(V) ( $Q_m = 2.350 \text{ mmol/g}$  for Cr(VI) and  $0.346 \text{ mmol/g}$  for As(V)). These values are comparable with the removal capacities of anion exchange fibers (Cr(VI) = 1.680–4.366 mmol/g; As(V) = 0.167–2.941 mmol/g) reported in the literature (Table 3) [13,15,20,25, 26,37,40–42].

Kinetic sorption data were analyzed by the kinetic sorption models including the pseudo first-order [Eq. (7)], pseudo second-order [Eq. (8)], and Elovich [Eq. (9)] models. Kinetic data along with the model fits for Cr(VI) and As(V) are presented in Figs. 6c and 6d, respectively. The removal of Cr(VI) and As(V) by the SA2 through the anion exchange was relatively fast. The Cr(VI) removal reached equilibrium within 15 min, whereas the As(V) removal reached equilibrium within 30 min. The corresponding model parameters are provided in Table 4. The values of  $R^2$ ,  $\lambda^2$ , and SAE indicated that the pseudo second-order model was better at describing the equilibrium data. The parameters values from the pseudo second-order model were  $q_e = 0.197 \text{ L/g}$  for Cr(VI) and  $q_e = 0.119 \text{ L/g}$  for As(V). The Cr(VI) removal rate was faster than that of As(V) ( $k_2 = 11.610 \text{ g/mol/min}$  for Cr(VI) and  $k_2 = 4.138 \text{ g/mol/min}$  for As(V)).

The effect of competing anions on the removal of Cr(VI) and As(V) is shown in Fig. 7. In the case of Cr(VI) (Fig. 7a), the effect of  $\text{Cl}^-$  and  $\text{NO}_3^-$  on the Cr(VI) removal was negligible; the values of  $R_e$  were 0.04 and 0.08%, respectively. The effects of  $\text{SO}_4^{2-}$  and  $\text{HPO}_4^{2-}$  on the Cr(VI) removal were very low; the values of  $R_e$  were 2.4 and 3.2%, respectively. Meanwhile, the effects of competing anions on the As(V) removal were noticeable (Fig. 7b). The values of  $R_e$  for  $\text{Cl}^-$  and  $\text{NO}_3^-$  were 15.5 and 27.1%, respectively. In addition, the values of  $R_e$  for  $\text{SO}_4^{2-}$  and  $\text{HPO}_4^{2-}$  were 76.6 and 64.1%, respectively. The influence of competing anions on the As(V) removal was with the decreasing order of  $\text{SO}_4^{2-} > \text{HPO}_4^{2-} > \text{NO}_3^- > \text{Cl}^-$ .

Regeneration and reuse of the fibers after the removal experiments is presented in Fig. 8. During the five regeneration and reuse cycles, the percent removal for Cr(VI) was 82.3–98.8%, whereas the percent removal for As(V) was 80.7–90.7%. These results demonstrated that the fibers can be successfully regenerated with NaCl solution.

### 3.6. Simultaneous removal of Cr(VI) and As(V) in mineral processing wastewater

Simultaneous removal of Cr(VI) and As(V) in mineral processing wastewater is presented in Fig. 9. The Cr(VI) removal rates were 5.2–52.7%, increasing with increasing fiber dosages from 2 to 20 g/L. The As(V) removal rates also increased from 2.9–22.8% with increasing fiber dosages from 2 to 20 g/L. The Cr(VI) removal capacities decreased from 3.098 to 1.587 mmol/g with increasing fiber dosages from 2 to 20 g/L, whereas the As(V) removal capacities

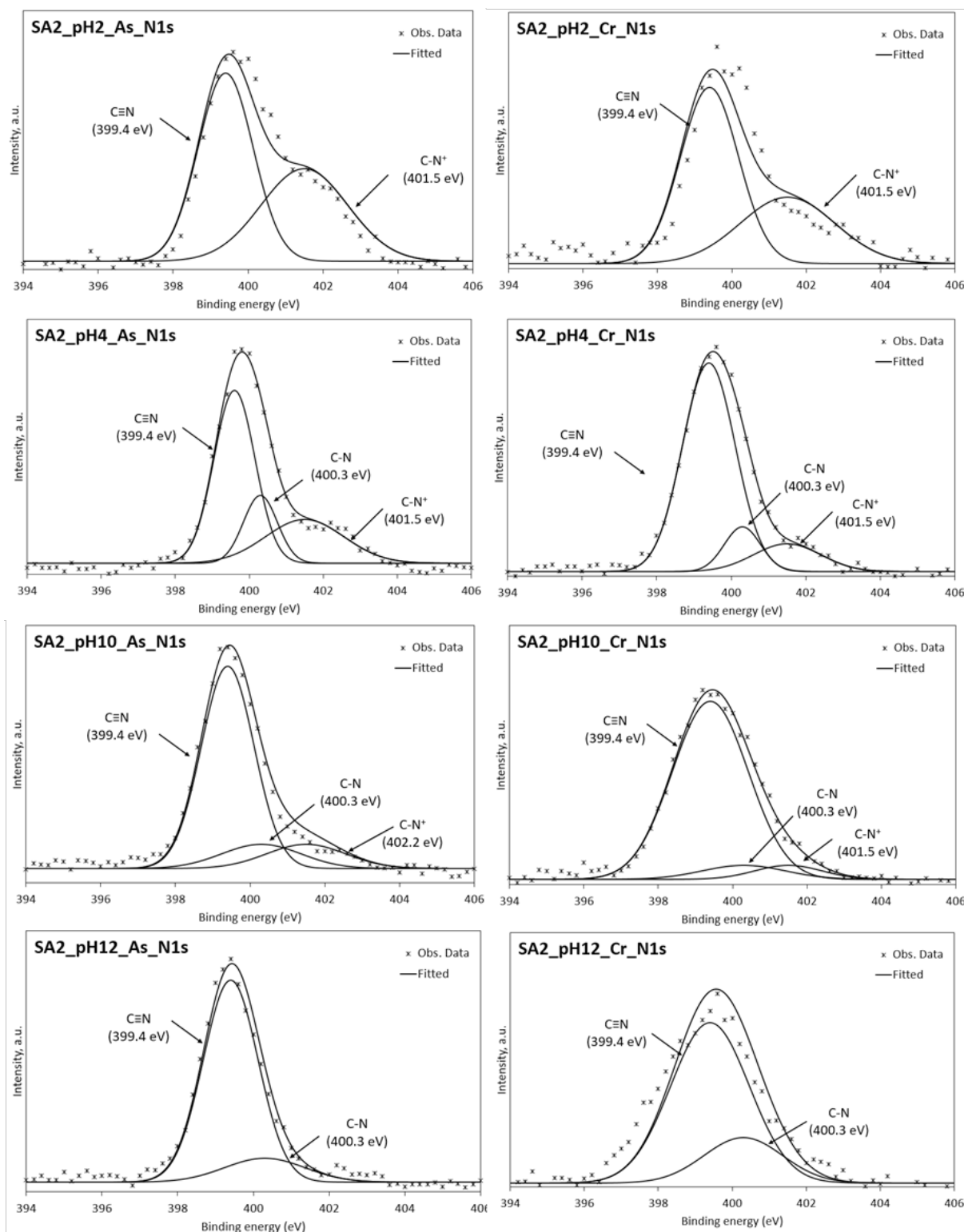


Fig. 5. Effect of solution pH on the high-resolution scan in the N1s region in the XPS spectra of the SA2.

decreased from 2.124 to 0.042 mmol/g at the same fiber dosages. At the given wastewater conditions (pH = 2.9; Cr(VI) concentration = 60.2 mmol/L; As(V) concentration = 67.5 mmol/L), the removal of Cr(VI) by the fiber was greater

than that of As(V). For instance, the Cr(VI) removal capacity at the fiber dosage of 10 g/L was 1.758 mmol/g with a 29.2% removal rate, whereas the As(V) removal capacity was 0.048 mmol/g with a 6.5% removal rate.

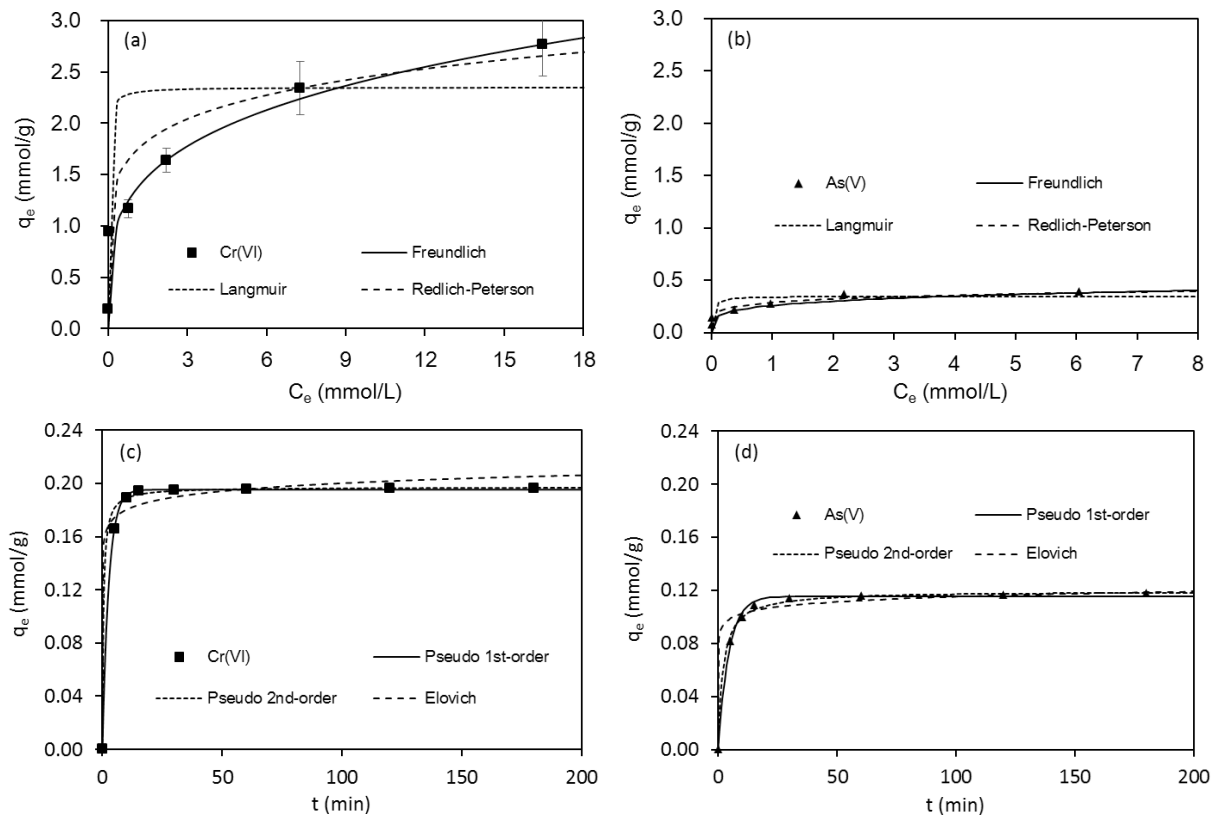


Fig. 6. Equilibrium and kinetic sorption data and nonlinear regression fits: (a) equilibrium data for Cr(VI), (b) equilibrium data for As(V), (c) kinetic data for Cr(VI), and (d) kinetic data for As(V). Equilibrium and kinetic model parameters are provided in Tables 2 and 4, respectively.

Table 2  
Equilibrium isotherm parameters obtained from the model fitting to equilibrium data

	Freundlich isotherm					Langmuir isotherm					Redlich-Peterson isotherm						
	$K_F$ (L/g)	$1/n$	$R^2$	$\chi^2$	SAE	$Q_m$ (mmol/g)	$K_L$ (L/mmol)	$R^2$	$\chi^2$	SAE	$K_R$ (L/g)	$a_R$ (L/mmol)	$K_R/a_R$ (mmol/g)	$g$	$R^2$	$\chi^2$	SAE
Cr(VI)	1.336	0.260	0.954	0.557	0.725	2.350	43.256	0.678	0.847	2.278	198.12	114.36	1.732	0.847	0.922	0.271	1.132
As(V)	0.258	0.214	0.965	0.018	0.098	0.346	40.273	0.784	0.067	0.255	56.61	196.14	0.289	0.847	0.963	0.015	0.115

Table 3  
Cr(VI) and As(V) removal capacities of anion exchange fibers reported in the literature

Anion exchange fiber	pH	Removal capacity (mmol/g)	Reference
SA2 fiber	4.3–5.1	Cr(VI), 2.350	This study
Polypyrrole-polyaniline nanofiber	2.0	Cr(VI), 4.366	[37]
QAPPS fiber	3.5	Cr(VI), 3.199	[40]
SAAEF fiber	1.0	Cr(VI), 3.610	[41]
SA fiber	4.0	Cr(VI), 1.680	[20]
SA2 fiber	7.5–8.6	As(V), 0.346	This study
Polyethylene/polypropylene quaternized fiber	7.0	As(V), 1.112	[25]
Coconut coir pith-based fiber	7.0	As(V), 0.167	[13]
Cellulose-based aminated fiber	6.0	As(V), 2.497	[15]
Cellulose-based fiber	6.0	As(V), 1.451	[42]
KC31	7.5–8.6	As(V), 2.941	[26]



Table 4  
Kinetic sorption parameters obtained from the model fitting to kinetic data

	Pseudo first-order model				Pseudo second-order model				Elovich						
	$q_e$ (mmol/g)	$k_1$ (1/min)	$R^2$	$\chi^2$	SAE	$q_e$ (mmol/g)	$k_2$ (g/mol/ min)	$R^2$	$\chi^2$	SAE	$\alpha$ (mmol/ min/g)	$\beta$ (g/mmol)	$R^2$	$\chi^2$	SAE
Cr(VI)	0.195	0.379	0.993	0.0004	0.004	0.197	11.610	0.994	0.0001	0.003	$5.52 \times 10^4$	179.72	0.766	0.0036	0.033
As(V)	0.116	0.224	0.964	0.0005	0.015	0.119	4.138	0.978	0.0003	0.010	$9.74 \times 10^5$	115.61	0.537	0.0022	0.048

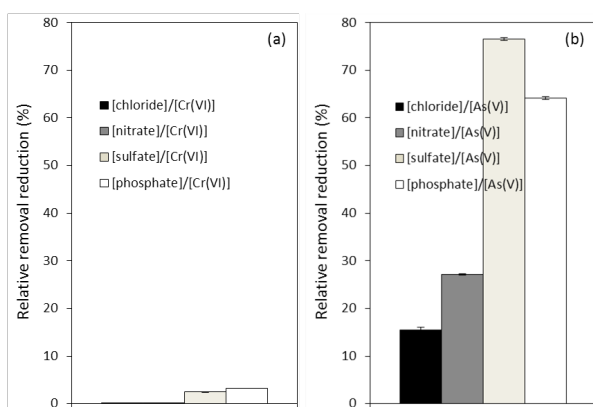


Fig. 7. Effect of competing anions on the removal of (a) Cr(VI) and (b) As(V).

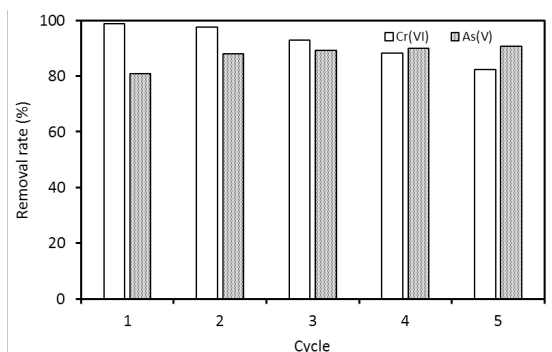


Fig. 8. Effect of regeneration and reuse on the removal rate of Cr(VI) and As(V) through five removal cycles.

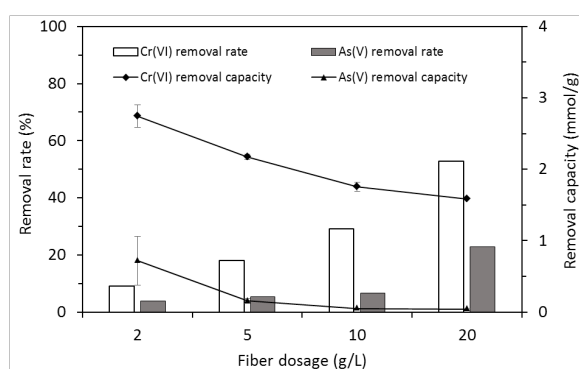


Fig. 9. Simultaneous removal rate and capacity of Cr(VI) and As(V) by the SA2 from mineral processing wastewater.

#### 4. Conclusions

The SA2 was used as the anion exchange fiber for the removal of Cr(VI) and As(V) in this study. Batch experiments indicated that the maximum removal capacities for Cr(VI) and As(V) were 2.350 and 0.346 mmol/g, respectively. The fiber was successfully regenerated with NaCl solution. The dependency of Cr(VI) and As(V) removal on the solution pH could be ascribed to both the number of protonated amines available for anion exchange and speciation of Cr(VI) and As(V) ions in response to pH change. XPS spectra demonstrated that the C-N<sup>+</sup> peak was prominent at pH 2 but disappeared as the pH increased to 12. Simultaneous removal experiments in the waste water showed that Cr(VI) removal by the fiber was more favorable than that of As(V). This study demonstrates that the SA2 could be applied for the treatment of Cr(VI) and As(V) in mineral processing wastewater.

#### Acknowledgment

This research is supported by the Korea Ministry of Environment as an Advanced Technology Program for Environmental Industry (Grant no. 2016000140011).

#### Symbols

- $a$  — Dose of anion exchange fiber
- $a_R$  — Redlich-Peterson constant related to the affinity of the ion exchange sites
- $C_e$  — Equilibrium concentration of contaminant in the aqueous phase
- $C_f$  — Concentration of contaminant in the aqueous phase after reaction
- $C_i$  — Concentration of contaminant in the aqueous phase before reaction
- $g$  — Redlich-Peterson constant related to the removal intensity
- $k_1$  — Pseudo first-order rate constant
- $k_2$  — Pseudo second-order rate constant
- $K_F$  — Freundlich constant related to the removal capacity
- $K_L$  — Langmuir constant related to the affinity of the exchange sites
- $K_R$  — Redlich-Peterson constant related to the removal capacity
- $1/n$  — Freundlich constant related to the removal intensity
- $Q_m$  — Maximum removal capacity
- $q_t$  — Amount of contaminant removed at time  $t$
- $q_w$  — Removal capacity in the presence of competing anion

- $q_{w/o}$  — Removal capacity in the absence of competing anion
- $R^2$  — Determination coefficient
- SAE — Sum of the absolute error
- $y_c$  — Removal capacity calculated from the model
- $\bar{y}_e$  — Removal capacity measured from the experiment
- $\underline{y}_e$  — Average measured removal capacity
- $\chi^2$  — Chi-square coefficient

## References

- [1] W.W. Eckenfelder, D.L. Ford, A.J. Englande, Industrial water quality, 4<sup>th</sup> Ed., The McGraw-Hill Companies, New York, 2009.
- [2] A. Zhitkovich, Chromium in drinking water: sources, metabolism, and cancer risks, *Chem. Res. Toxicol.*, 24 (2011) 1617–1629.
- [3] S.K. Sharma, B. Petrusovski, G. Amy, Chromium removal from water: a review, *J. Water Supply Res. Technol.-Aqua*, 57 (2008) 541–553.
- [4] A.M. Nazari, R. Radzinski, A. Ghahreman, Review of arsenic metallurgy: treatment of arsenical minerals and the immobilization of arsenic, *Hydrometallurgy*, 174 (2017) 258–281.
- [5] A.K. Sengupta, D. Clifford, S. Subramonian, Chromate ion-exchange process at alkaline pH, *Water Res.*, 20 (1986) 1177–1184.
- [6] S. Mustafa, H. Bashir, N. Rehana, A. Naeem, Selectivity reversal and dimerization of chromate in the exchanger Amberlite IRA-400, *React. Func. Polym.*, 34 (1997) 135–144.
- [7] V. Neagu, I. Untea, E. Tudorache, C. Luca, Retention of chromate ion by conventional and N-ethylpyridinium strongly basic anion exchange resins, *React. Func. Polym.*, 57 (2003) 119–124.
- [8] B. Galán, D. Castañeda, I. Ortiz, Removal and recovery of Cr(VI) from polluted ground waters: A comparative study of ion-exchange technologies, *Water Res.*, 39 (2005) 4317–4324.
- [9] B. Mukhopadhyay, J. Sundquist, E. White, Hydro-geochemical controls on removal of Cr(VI) from contaminated groundwater by anion exchange, *Appl. Geochem.*, 22 (2007) 370–387.
- [10] T. Shi, Z. Wang, Y. Liu, S. Jia, D. Changming, Removal of hexavalent chromium from aqueous solutions by D301, D314 and D354 anion-exchange resins, *J. Hazard. Mat.*, 161 (2009) 900–906.
- [11] M.M. El-Moselhy, O.M. Hakami, Selective removal of chromate using hybrid anion exchanger, *Desal. Water Treat.*, 56 (2015) 2917–2924.
- [12] J. Kim, M.M. Benjamin, Modeling a novel ion exchange process for arsenic and nitrate removal, *Water Res.*, 38 (2004) 2053–2062.
- [13] T.S. Anirudhan, M.R. Unnithan, Arsenic(V) removal from aqueous solutions using an anion exchanger derived from coconut coir pith and its recovery, *Chemosphere*, 66 (2007) 60–66.
- [14] M.R. Awual, A. Jyo, Rapid column-mode removal of arsenate from water by cross linked poly (allylamine) resin, *Water Res.*, 43 (2009) 1229–1236.
- [15] T.S. Anirudhan, S. Jalajamony, Cellulose-based anion exchanger with tertiary a mine functionality for the extraction of arsenic(V) from aqueous media, *J. Environ. Manage.*, 91 (2010) 2201–2207.
- [16] M.R. Awual, M.A. Hossain, M.A. Shenashen, T. Yaita, S. Suzuki, A. Jyo, Evaluating of arsenic(V) removal from water by weak-base anion exchange adsorbents, *Environ. Sci. Pollut. Res.*, 20 (2013) 421–430.
- [17] M. Kukučka, N. Kukučka, M. Vojnović-Miloradov, Ž. Tomić, M. Šiljeg, Effect of extremely high specific flow rates on the removal of NOM and arsenic from groundwater with an ion-exchange resin: A pilot-scale study in Northern Serbia, *J. Environ. Sci. Health A Tox. Hazard. Subst. Environ. Eng.*, 46 (2011) 952–959.
- [18] E.G. Kosandrovich, V.S. Soldatov, Fibrous Ion Exchangers, In: Dr. I., Luqman, M. (Ed.), *Ion Exchange Technology I: Theory and Materials*, Springer Netherlands, Dordrecht, 2012, pp. 299–371.
- [19] L. Dai, L. Cui, D. Zhou, J. Huang, S. Yuan, Resource recovery of Cr(VI) from electroplating wastewater: Laboratory and pilot-scale investigation using fibrous weak anion exchanger, *J. Taiwan Inst. Chem. Eng.*, 54 (2015) 170–177.
- [20] C.G. Lee, J.A. Park, J.W. Choi, S.O. Ko, S.H. Lee, Removal and recovery of Cr(VI) from industrial plating wastewater using fibrous anion exchanger, *Water Air Soil Pollut.*, 227 (2016) 287–297.
- [21] S.C. Lee, J.K. Kang, E.H. Sim, N.C. Choi, S.B. Kim, Modacrylic anion exchange fibers for Cr(VI) removal from chromium-plating rinse water in batch and flow-through column experiments, *J. Environ. Sci. Health A Tox. Hazard. Subst. Environ. Eng.*, 52 (2017) 1195–1203.
- [22] L. Ruixia, G. Jinlong, T. Hongxiao, Adsorption of fluoride, phosphate, and arsenate ions on a new type of ion exchange fiber, *J. Colloid Interface Sci.*, 248 (2002) 268–274.
- [23] L. Dominguez, J. Economy, K. Benak, C.L. Mangun, Anion exchange fibers for arsenate removal derived from a vinylbenzyl chloride precursor, *Polym. Adv. Technol.*, 14 (2003) 632–637.
- [24] M.R. Awual, S. Urata, A. Jyo, M. Tamada, A. Katakai, Arsenate removal from water by a weak-base anion exchange fibrous adsorbent, *Water Res.*, 42 (2008) 689–696.
- [25] C. Kavaklı, P.A. Kavaklı, B.D. Turan, A. Hamurcu, O. Güven, Quaternizeddimethylaminoethyl methacrylate strong base anion exchange fibers for As(V) adsorption, *Radiat. Phys. Chem. Oxf. Engl.*, 1993, 102 (2014) 84–95.
- [26] S.C. Lee, J.K. Kang, E.H. Sim, N.C. Choi, S.B. Kim, As(V) removal from arsenic wastewater by fibrous anion exchangers, *Desal. Water Treat.*, 90 (2017) 273–282.
- [27] P.V. Nesteronok, V.S. Soldatov, Acid–base properties of ion exchangers: V. Synthesis and properties of ion exchangers on the base of modacrylic polyacrylonitrile–vinylchloride fibers, *React. Function. Polym.*, 71 (2011) 1033–1039.
- [28] V. Neagu, S. Mikhailovsky, Removal of hexavalent chromium by new quaternized crosslinked poly (4-vinylpyridines), *J. Hazard. Mater.*, 183 (2010) 533–540.
- [29] J.P. Coates, A practical approach to the interpretation of infrared spectra, In: R.A. Meyers, (Ed.), *Encyclopedia of Analytical Chemistry*, Ó John Wiley & Sons Ltd UK, Chichester, 2000, pp. 10815–10837.
- [30] G. Li, J. Xiao, W. Zhang, Efficient and reusable a mine-functionalized polyacrylonitrile fiber catalysts for Knoevenagel condensation in water, *Green Chem.*, 14 (2012) 2234–2242.
- [31] Y. Turhan, M. Dogan, M. Alkan, Poly(vinyl chloride)/Kaolinite nanocomposites: Characterization and thermal and optical properties, *Ind. Eng. Chem. Res.*, 49 (2010) 1503–1513.
- [32] S.M. Ashraf, A laboratory manual of polymers, IK International Publishing House Pvt. Ltd India, New Delhi, 2008.
- [33] M. Koyama, Y. Tsujizaki, S. Sakamuram, New amides from buckwheat seeds (*Fagopyrum esculentum* Moench), *Agric. Biol. Chem.*, 37 (1973) 2749–2753.
- [34] Y.G. Ko, U.S. Choi, T.Y. Kim, D.J. Ahn, Y.J. Chun, FT-IR and isotherm study on anion adsorption onto novel chelating fibers, *Macromol. Rapid Commun.*, 23 (2002) 535–539.
- [35] D.H. Shin, Y.G. Ko, U.S. Choi, W.N. Kim, Design of high efficiency chelate fibers with an a mine group to remove heavy metal ions and pH-related FT-IR analysis, *Ind. Eng. Chem. Res.*, 43 (2004) 2060–2066.
- [36] P. Lakshminathiraj, B.R.V. Narasimhan, S. Prabhakar, G.B. Raju, Adsorption studies of arsenic on Mn-substituted iron oxyhydroxide, *J. Colloid Interf. Sci.*, 304 (2006) 317–322.
- [37] M. Bhaumik, A. Maity, V.V. Srinivasu, M.S. Onyango, Removal of hexavalent chromium from aqueous solution using polypyrrole-polyaniline nanofibers, *Chem. Eng. J.*, 181/182 (2012) 323–333.
- [38] W. Zheng, J. Hu, Z. Han, E. Diesel, Z. Wang, Z. Zheng, C. Ba, J. Langer, J. Economy, Interactions of Cr(VI) with hybrid anion exchange/porous carbon fibers in aqueous solution at natural pH, *Chem. Eng. J.*, 287 (2016) 54–61.
- [39] D.Q.L. Oliveira, M. Gonçalves, L.C.A. Oliveira, L.R.G. Guilherme, Removal of As(V) and Cr(VI) from aqueous solutions using solid waste from leather industry, *J. Hazard. Mater.*, 151 (2008) 280–284.

- [40] J. Huang, X. Zhang, L. Bai, S. Yuan, Polyphenylene sulfide based anion exchange fiber: Synthesis, characterization and adsorption of Cr(VI), *J. Environ. Sci.*, 24 (2012) 1433–1438.
- [41] W. Wang, M. Li, Q. Zeng, Thermodynamics of Cr(VI) adsorption on strong alkaline anion exchange fiber, *Trans. Nonferrous Met. Soc. China.*, 22 (2012) 2831–2839.
- [42] T.S. Anirudhan, J. Nima, S. Sandeep, V.R.N. Ratheesh, Development of an amino functionalized glycidylmethacrylate-grafted-titanium dioxide densified cellulose for the adsorptive removal of arsenic (V) from aqueous solutions, *Chem. Eng. J.*, 209 (2012) 362–371.